

Influence of modern magnetic and insulation materials on dimensions and losses of large induction machines

François Balavoine, Bertrand Cassoret, Cristian Demian, Raphael Romary, Christophe Debendere

▶ **To cite this version:**

François Balavoine, Bertrand Cassoret, Cristian Demian, Raphael Romary, Christophe Debendere. Influence of modern magnetic and insulation materials on dimensions and losses of large induction machines. Open Physics, 2020, 18 (1), pp.652-657. 10.1515/phys-2020-0172 . hal-03253693

HAL Id: hal-03253693
https://univ-artois.hal.science/hal-03253693

Submitted on 3 Oct 2022

HAL is a multi-disciplinary open access archive for the deposit and dissemination of scientific research documents, whether they are published or not. The documents may come from teaching and research institutions in France or abroad, or from public or private research centers.

L'archive ouverte pluridisciplinaire **HAL**, est destinée au dépôt et à la diffusion de documents scientifiques de niveau recherche, publiés ou non, émanant des établissements d'enseignement et de recherche français ou étrangers, des laboratoires publics ou privés.

Research Article

Balavoine François*, Cassoret Bertrand, Demian Cristian, Romary Raphaël, and Debendere Christophe

Influence of modern magnetic and insulation materials on dimensions and losses of large induction machines

https://doi.org/10.1515/phys-2020-0172
received March 13, 2020; accepted June 29, 2020

Abstract: The aim of this study is to present the possibilities of reducing the size of large induction motors with new electrical materials taken into account of thermal constraints. This study highlights the possibilities of reducing losses, increasing the efficiency, and decreasing the weight, by taking different grades of materials. A nonlinear multiobjective optimization is used to determine the best solution, by varying the internal and external geometric parameters.

Keywords: Induction motor, magnetic sheets, insulation, motor design, electrical materials

List of symbols

- A_l: specific current loading (A/m)
- $\hat{B}$: flux density (T)
- $\hat{B}_e$: air gap flux density (T)
- C_{mec}: machine sizing constant (kW s/m^3)
- cos ϕ: power factor
- D: internal diameter motor (m)
- η: efficiency
- H: magnetic field (A/m)
- K_{w1}: winding factor
- L: length motor (m)
- n: speed revolutions per second) (rps)
- p: pole pair numbers
- P_{Cu}: copper losses (W)
- P_{mec}: mechanical power (W)
- P_{Iron}: iron losses (W)
- Rad$_i$: radius of different stator parts (m)
- S: apparent power (VA)
- T_l: critical temperature point (°C)

1 Introduction

A plenty of medium and large power induction machines (IMs) manufactured in the first half of the 1900s are still in operation today [1]. It is possible to improve efficiency, reduce volume, or both by replacing insulation or magnetic sheets with current, modern materials [2]. The aim of this study is to quantify the influence of the materials on the dimensions of different IMs at given rated power from 1950s to present days and to present the contribution of new materials to performance improvements. This step allows us to reduce the size of the machines. This work is based on classical methods of sizing literature.

The main dimensions of the IM are essentially related to the power density coefficient C_{mec}, in kW s/m^3 [3]. This quantity depends on the specific current loading A_l in A/m, the air gap flux density $\hat{B}_e$ in T, and the winding factor K_{w1}. Equations 1 and 2 give the mechanical power P_{mec} in kW, which is proportional to C_{mec}. Independently of the speed and thus the pole number, the constant C_{mec} provides the main dimension of the machine. Figure 1 presents the evolution at different periods of this constant for pole pair numbers from two to six. The curves allow one to deduce the evolution of the inner stator diameter and length at given speed [4,5]. This evolution shows that the

* **Corresponding author: Balavoine François,** Univ. Artois, UR 4025, Laboratoire Systèmes Electrotechniques et Environnement (LSEE), Béthune, F-62400, France,
e-mail: francois.balavoine@univ-artois.fr
Cassoret Bertrand, Demian Cristian, Romary Raphael: Univ. Artois, UR 4025, Laboratoire Systèmes Electrotechniques et Environnement (LSEE), Béthune, F-62400, France
Debendere Christophe: Flipo Richir, Seclin, F-59473, France,
e-mail: christophe.debendere@flipo-richir.com

Open Access. © 2020 Balavoine François *et al.*, published by De Gruyter. This work is licensed under the Creative Commons Attribution 4.0 International License.

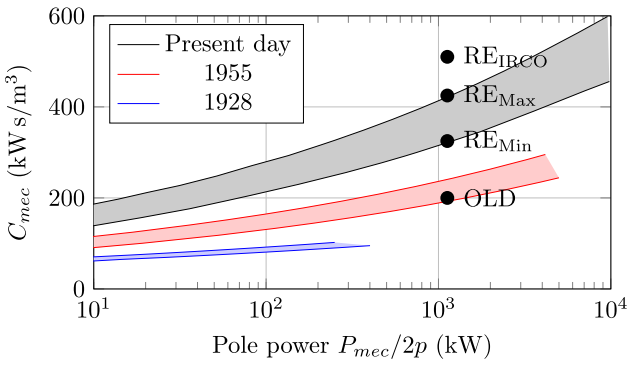


Figure 1: Evolution of machine sizing constant C_{mec} based on empirical knowledge and a traditional know-how, for pole pairs two to six.

machines are getting smaller and smaller in size for the same power:

$$P_{mec} = \frac{\pi^2}{\sqrt{2}} \cdot K_{w1} \cdot A_l \cdot \hat{B}_e \cdot D^2 \cdot L \cdot n \cdot \cos\phi \cdot \eta, \quad (1)$$

$$P_{mec} = C_{mec} \cdot D^2 \cdot L \cdot n, \quad (2)$$

$$C_{mec} = \frac{\pi^2}{\sqrt{2}} \cdot K_{w1} \cdot A_l \cdot \hat{B}_e \cdot \cos\phi \cdot \eta. \quad (3)$$

Section 2 of this study deals with the improvement of IM motors and give the details of the impact of electrical insulation and magnetic circuit quality. In order to check the critical temperature points, Section 3 presents a simplified thermal circuit model. Section 4 deals with the choice of a 4.5 MW IM and gives the first results. Section 5 presents the optimization and dimensions of the best case and a conclusion.

2 Improvement of the IM

2.1 Presentation of the studied machine

The study focuses on the design of a 4.5 MW, two pole pairs, a 6.6 kV voltage supply IM. This is a squirrel cage machine with 72 stator slots and 62 rotor slots. Four different configurations with the same airgap width have been studied as follows:

1) Old electrical insulation and old magnetic circuit with C_{mec} = 200 kWs/m^3 (named OLD),
2) Recent (RE) materials, minimum value of C_{mec} = 325 kWs/m^3 (named RE_{Min}),
3) Recent materials, maximum value of C_{mec} = 425 kWs/m^3 (named RE_{Max}),
4) Recent materials, iron cobalt electrical steel sheets, and high value of C_{mec} = 510 kWs/m^3 (named RE_{IRCO}).

The three values of C_{mec} come from usual design, whereas the last one corresponds to the size reduction target.

2.2 Impact of electrical insulation

The electrical insulation evolution allows the increase of the dielectric strength and the acceptable temperature. This concerns the high voltage insulation and the fill factor improvement of copper in the slots [1,6].

Tables 1 and 2 give an overview about the improvement of electrical insulation. It can be seen in Table 1 that before 1960s the groundwall insulation was essentially made of micanite tube, which is an assembly of thin flakes of mica stuck together with a flexible varnish. The tube thickness depends on voltage supply. The conductor insulation was composed of various papers and cotton. A few turns around the conductors were necessary.

The new electrical insulations presented in Table 2 are composed of several types of thin materials, each brings a specific insulation function in the IM (turn-to-turn insulation, corona effect, and mechanical protection). To the nearest of the conductor, the turn-to-turn protection is a base of mica paper with epoxy resin impregnation.

Table 1: Old electrical insulation

Localization	Years	Width (mm)	Composition
Flat copper	1926/1928	0.4	Cotton wrapping or tape paper
	1955	0.3–0.4	
Winding/groundwall	1926/1928	2.5–4	Micanite sheath/tube
	1955	2.5–3	

Table 2: Recent electrical insulation

Localization	Width (mm)	Composition/laminating
Flat copper[a]	0.3	Mica tape with polyester film
Winding[b]	0.15	Mica paper with metallic salt accelerator and zinc naphthenate
Groundwall[c]	0.085	Conductor tape with polyester tape
Corona effect		
Groundwall[d]	0.18	Glass and polyester and polyester felt with epoxy resin
Finish tape		
Total[e]	0.415	Total insulation for the coil winding and groundwall
Winding + groundwall		

[a] It is the insulation closest to the copper conductor; [b] The insulation of the winding, i.e. of all the conductors; [c] It is one of the groundwall insulations, for the corona effect; [d] It is second of the groundwall insulations (for mechanical protection); [e] It is the sum of the dimensions of the groundwall + winding insulation, for the coil insulation (without flat cooper).

2.3 Impact of magnetic circuit quality

The electrical steel sheet quality has been improved through a better building process. Among the non-oriented steel sheet, the following three categories based on datasheet have been considered:

- old iron silicon sheets (thickness 0.5 mm or 1 mm) (taken as a reference),
- recent iron silicon sheets (thickness 0.5 mm), and
- recent iron cobalt sheets (thickness 0.35 mm).

These materials are described in Figures 2 and 3 [7–9].

Among the electrical steel sheet qualities used in the paper, the lowest losses are for iron cobalt called iron and cobalt conception (IRCO). Their losses are around 1.4 W/kg at 1.5 T and 50 Hz [10], whereas those of the old sheets are between 6 and 8 W/kg.

This steel sheet is characterized by a high saturation induction at 2.3 T, whereas the others have a weaker saturation level at 1.8 T. Moreover, the difference in the bend of the curve is more important for the old characteristics [11].

3 Simplified thermal circuit model

In order to optimize the size of IM, the thermal circuit model allows one to check the temperature within the IM. The critical temperature point at the surface of the conductors in the stator slots and in the end windings is well known. Joule and magnetic losses will be the main cause of temperature increase in the machine.

The selected thermal model considers only the heat transfer by radial conduction within the machine. The use of thermal potential differences will allow us to evaluate the temperature increase at different points of the machine. The thermal model (Figures 4 and 5) will be in a steady state operating condition of the machine [12].

In the thermal network, two power sources are considered in this circuit, the Joule and iron losses in the stator. The variables T_i correspond to the temperature at different points in the stator. The thermal resistances of this network are calculated from the analytical equations of the heat equations at the area borders defined by the radius Rad_i in Figure 5. They depend on geometrical parameters and the material thermal conductivity. The resistances are calculated at different points of the winding, insulation, stator yoke, and the frame in contact with the ambient air.

The thermal conductivities used in the model are as follows [12]:

- Coil 5 W/(mK);
- Winding insulators 0.20 W/(mK);
- Iron and silicon magnetic circuit 25 W/(mK); and
- Cast-iron housing 52 W/(mK).

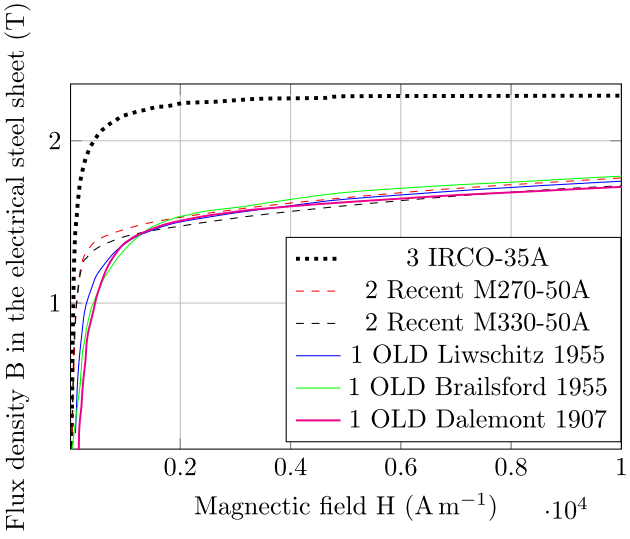


Figure 2: Electrical steel sheets quality comparison of B–H curves.

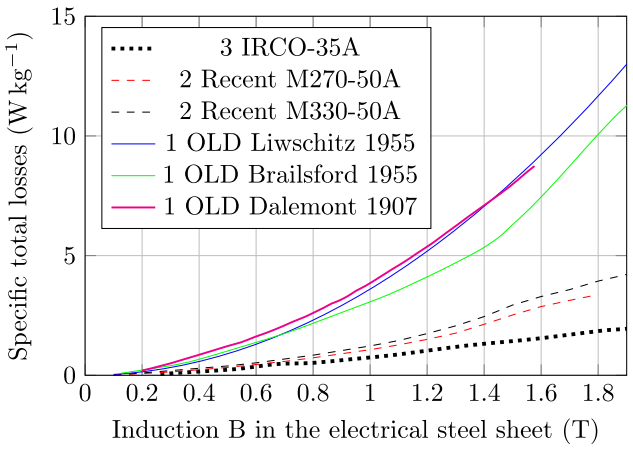


Figure 3: Electrical steel sheets quality comparison of specific total losses.

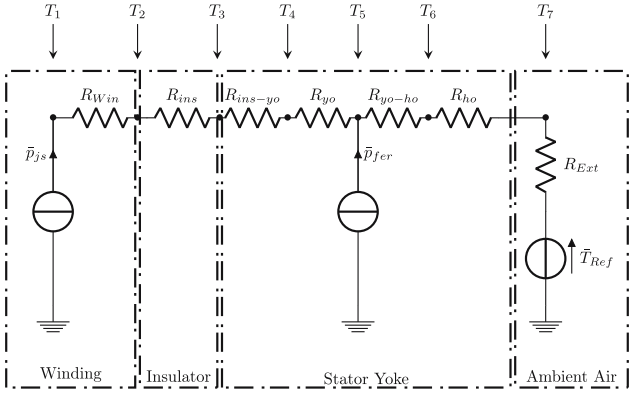


Figure 4: Simplified thermal circuit model.

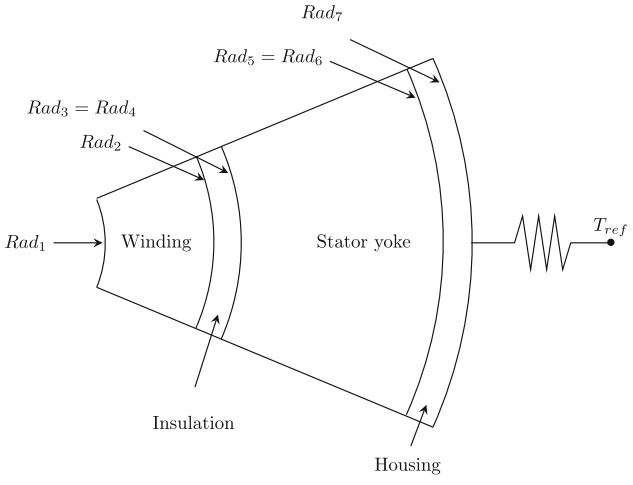


Figure 5: Simplified stator for the thermal model.

4 Main dimensions and results

The sizing approach is based on the usual equations of large IM design [4,5]. This is a traditional approach that enables us to obtain a fast dimensioning of the machine, but that suffers of a lack of accuracy for loss determination. However, the used method gives tendencies about the influence of modern materials on the sizing.

Partial results are presented in Table 3 that gives the main dimensions for each configuration, based on Figure 1 for C_{mec} and considering material characteristics.

For RE_{IRCO}, the constant C_{mec} is chosen to be 510 kW s/m^3 higher than the present day area of Figure 1 corresponding to the gray area between RE_{Min} and RE_{Max}.

The results of the design process show that for the same rated power, the air gap flux density is slightly higher for the machine with IRCO because the magnetomotive force losses in the material are lower.

Figure 6 gives the efficiency of each machine resulting from analytical calculations. The results show an improvement of efficiency between the old and the new materials. The results in Figure 7 show a decrease of 52.3% for iron weight, 15.8% for copper weight, and 0.54 point efficiency rise, between the OR_old and the best IM

Table 3: Principal internal dimensions for 4.5 MW IM

IM	Inner diameter (m)	Outer diameter (m)	Iron length (m)
OLD	1	1.57	0.9
RE_{Min}	0.8105	1.19	0.90
RE_{Max}	0.737	1.08	0.82
RE_{IRCO}	0.68	1.05	0.76

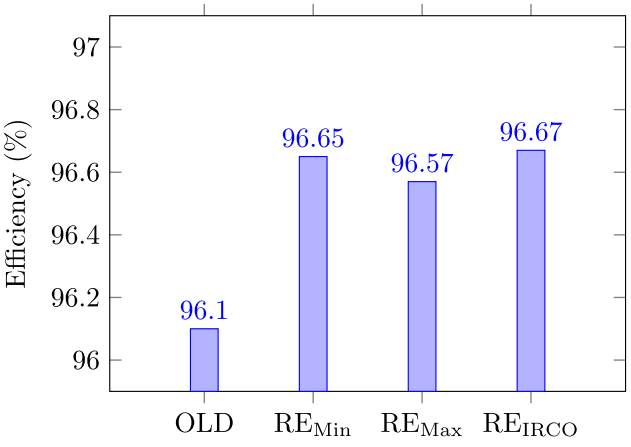


Figure 6: Efficiency of each configuration.

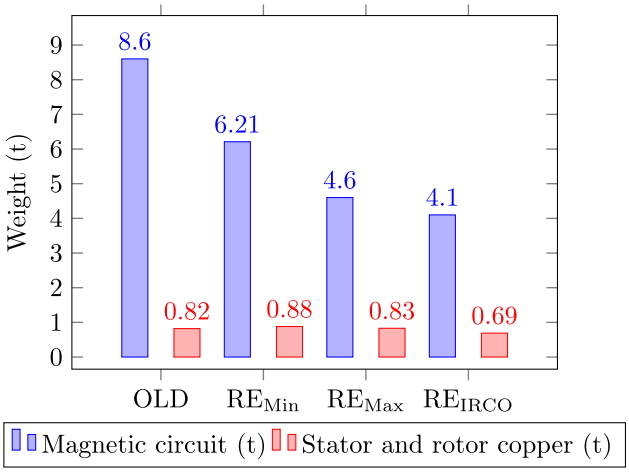


Figure 7: Weight of magnetic circuit and copper of each configuration.

Table 4: Main sources of thermal model and temperature of conductors inside the stator

IM	OLD	RE_{Min}	RE_{Max}	RE IRCO
P_{Cu} (kW)	28.8	24.4	22.4	27.2
P_{Iron} (kW)	38.4	12.85	16.6	11
T_1 (°C)	127	82.7	75.8	83.6

configuration (IRCO). However, for usual applications, the economic criteria lead to choose an iron-silicon magnetic circuit (cases RE_{Min} and RE_{Max}) instead of IRCO. Indeed, IRCO sheets can cost 5–10 times more than IRSI sheets. Concerning the efficiency, the improvement is roughly the same but the iron weight and volume are more reduced with IRCO.

Table 4 shows the copper losses (P_{Cu}) and iron losses (P_{Iron}) in the stator, which can be used for the thermal model. Then, the thermal circuit model gives the temperature T_1 for each machine, which corresponds to the critical point located at the conductor surface. Table 4 also presents the temperature T_1 for each machine. This table shows a reduction of local heating at the critical point, between the old and new configurations, caused by the insulation thickness improvement. The results related to the main losses and the temperature T_1 are consistent.

5 Optimization of IRCO case

This part presents the dimensioning of the machine using a genetic algorithm. The NSGA-II code is used with MATLAB in order to determine a set of results presented in the form of Pareto curve [13–15]. The previous configurations stem from datasheet curves of Figure 1. The design will ensure acceptable temperature, especially, in the recommended area between RE_{Min} and RE_{Max}. The aim of this section is to calculate and control the case IRCO outside this area.

In order to obtain optimized results for iron cobalt case, a nonlinear multiobjective optimization with analytical calculations is used ref. [16,17]. This optimization makes it possible to vary the main dimensions of the machine (diameter and length) and the size of stator slots. The main objective is the smallest dimensions with equivalent efficiency to this range of motors. The constraints used in this optimization define the physical limits that can be taken into account. These limits are as follows: the saturation of the magnetic induction at 2.2 T for iron cobalt electrical steel sheet, the magnetizing current, the current density in the winding, the maximum temperature inside a conductor and one mechanical constraint, corresponding to the shaft diameter chosen at 0.25 m for this power.

The variation in the input parameters in the genetic algorithm returns a matrix with several results depending on the objectives. This matrix shows a result set in Figure 8 in the form of a Pareto curve.

Based on this curve, it is possible to calculate the volume and choose a Pareto optimum. This point gives a shorter length and close diameters: the inner diameter is 0.684 m, the outer diameter 1.05 m, and the length is 0.66 m. The efficiency is 96.65%, almost the same as before (96.67%). The magnetic circuit weight is of 3.37 t a reduction of 17.1% compared to the

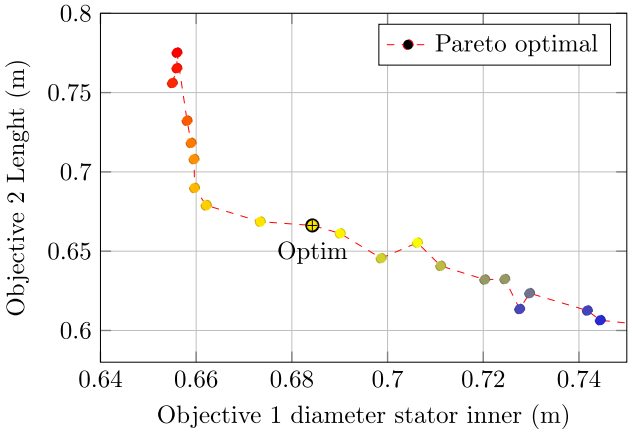


Figure 8: Pareto curve for two objectives about a design motor with iron cobalt electrical sheet steel.

Table 5: Comparison between two IRCO configurations

IM	RE IRCO	Optimization IRCO
η (%)	96.67	96.65
Weight of iron (t)	4.1	3.4
Weight of copper (t)	0.69	0.6
T_1 (°C)	83.6	90
P_{Cu} (kW)	27.2	31.8
P_{Iron} (kW)	11	11.7

RE_{IRCO} case and 0.6 t for stator and rotor copper, a reduction of 13%.

Comparing this solution with the previous RE_{IRCO} machine (Table 5), it can be noted that the lowest weight and dimensions are obtained with the same efficiency. The temperature increase is still acceptable. This new optimized design leads to C_{mec} = 580 kW s/m^3 instead of 510 kW s/m^3.

6 Conclusion and discussion

This paper presents a study about the building of IM at different periods. It shows how the electrical material ameliorations have an impact on the main dimensions, the weight, and the efficiency. The results show that for the best case with the iron cobalt magnetic circuit, an important reduction of internal diameter, length, and weight, and a 0.54 point efficiency improvement can be obtained. To specify the results and validate the IM size reduction, a thermal circuit model is exploited to check the temperature at the critical point T_1 located at the surface of the stator conductors. To improve the IM design, a genetic algorithm is used to find the best solution using the analytical relations and considering the thermal constraints. The geometric parameters of IM can be changed for different objectives, as minimizing weight while keeping a good efficiency. The optimization allows us to find the best solution into the Pareto matrix. The optimal weight reduction is 60.8% for magnetic circuit and 26.8% for total copper between case OLD and optimized IRCO.

References

[1] Stone G, Boulter E, Culbert I, Dhirani H. Electrical insulation for rotating machines: design, evaluation, aging, testing, and repair. vol. 21, Wiley-IEEE Press; 2004.

[2] Chiricozzi E, Parasiliti F, Villani M. New materials and innovative technologies to improve the efficiency of three-phase induction motors. a case study. 16th International Conference on Electrical Machines ICEM; 2004. p. 5–8.

[3] Boldea I, Nasar SA. The induction machines design handbook. CRC Press; 2018.

[4] Pyrhonen J, Jokinen T, Hrabovcova V. Design of rotating electrical machines. Wiley; 2013.

[5] Liwschitz M, Garik W. Electric Machinery, volume II of AC Machines. New York: D. Van Nostrand Company, Inc.; 1950.

[6] Gray A. Electrical machine design. New York: McGraw-Hill Book Company; 1926.

[7] Brailsford F, Bradshaw CG Iron losses at high magnetic flux densities in electrical sheet steels. Proc IEE – Part A: Power Eng. August 1955;102(4):463–71.

[8] Krings A. Iron losses in electrical machines-influence of material properties, manufacturing processes, and inverter operation, PhD dissertation. KTH Royal Institute of Technology; 2014.

[9] Tomczuk B, Koteras D. Magnetic flux distribution in the amorphous modular transformers. J Magn Magn Mater. 2011;323(12):1611–5.

[10] Bloch F, Waeckerle T, Fraisse H. The use of iron-nickel and iron-cobalt alloys in electrical engineering, and especially for electrical motors. 2007 Electrical Insulation Conference and Electrical Manufacturing Expo. IEEE; 2007. p. 394–401.

[11] Hihat N, Komeza K, Juszczak EN, Lecointe JP. Experimental and numerical characterization of magnetically anisotropic laminations in the direction normal to their surface. IEEE Trans Magn. 2011;47(11):4517–22.

[12] Hachicha MR, Ghariani M, Neji R. Thermal model for induction machine. Eighth International Multi-Conference on Systems, Signals Devices; March 2011. p. 1–5.

[13] Appelbaum J, Fuchs E, White J. Optimization of three-phase induction motor design part i: Formulation of the optimization technique,. IEEE Trans Energy Convers. 1987;3:407–14.

[14] Deb K. Multi-objective optimization using evolutionary algorithms. vol. 16, USA: Wiley-IEEE Press; 2001.

[15] Ranjan S, Mishra SK. Multi-objective design optimization of three-phase induction motor using nsga-ii algorithm. Computational Intelligence in Data Mining. vol. 2, Springer India; 2015. p. 1–8.

[16] Liuzzi G, Lucidi S, Parasiliti F, Villani M. Multiobjective optimization techniques for the design of induction motors. IEEE Trans Magn. May 2003;39(3):1261–4.

[17] Nangsue P, Pillay P, Conry SE. Evolutionary algorithms for induction motor parameter determination. IEEE Trans Energy Convers. Sep. 1999;14(3):447–53.